JOC Featured Article

pubs.acs.org/joc

Mutremdamide A and Koshikamides C−H, Peptide Inhibitors of HIV-1 Entry from Different *Theonella* Species

Alberto Plaza,[†] Giuseppe Bifulco,[‡] Milena Masullo,[‡] John R. Lloyd,[†] Jessica L. Keffer,[†] Patrick L. Colin,[§] John N. A. Hooper,[⊥] Lori J. Bell,[§] and Carole A. Bewley*[,†]

[†]*Laboratory of Bioorganic Chemistry, National Institute of Diabetes and Digestive and Kidney Diseases, National Institutes of Health, Bethesda, Maryland 20892,* [‡]*Dipartimento di Scienze Farmaceutiche, University of Salerno, Via Ponte Don Melillo, 84084 Fisciano, Salerno, Italy,* [§]*Coral Reef Research Foundation, Republic of Palau, and* [⊥]*Queensland Museum, P.O. Box 3300, South Brisbane, Qld 4101, Australia*

caroleb@mail.nih.gov.

Received January 17, 2010

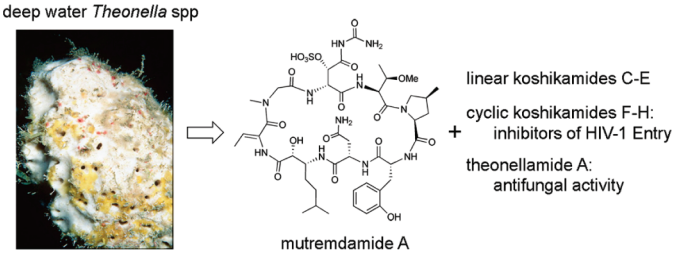

A new sulfated cyclic depsipeptide, termed mutremdamide A, and six new highly *N*-methylated peptides, termed koshikamides C−H, were isolated from different deep-water specimens of *Theonella swinhoei* and *Theonella cupola*. Their structures were determined using extensive 2D NMR, ESI, or CDESI and QTOF-MS/MS experiments and absolute configurations established by quantum mechanical calculations, advanced Marfey's method, and chiral HPLC. Mutremdamide A displays a rare 2-amino-3-(2-hydroxyphenyl)propanoic acid and a new N^{δ}-carbamoyl-β-sulfated asparagine. Koshikamides C−E are linear undecapeptides, and koshikamides F−H are 17-residue depsipeptides containing a 10-residue macrolactone. Koshikamides F and G differ from B and H in part by the presence of the conjugated unit 2-(3-amino-5-oxopyrrolidin-2-ylidene)propanoic acid. Cyclic koshikamides F and H inhibited HIV-1 entry at low micromolar concentrations while their linear counterparts were inactive. The *Theonella* collections studied here are distinguished by co-occurrence of mutremdamide A, koshikamides, and theonellamides, the combination of which appears to define a new *Theonella* chemotype that can be found in deeper waters.

Introduction

According to estimates from WHO, about 40 million people worldwide are infected with HIV and another 4 million new infections occur each year.[1] The increase in transmission of multidrug-resistant strains[2] warrants continued efforts to develop new HIV inhibitors that target specific events that are critical to viral replication. Marine sponges of the Lithistida order have shown to be an important source of nonribosomal peptides with unique structures and in some cases potent anti-HIV activity. A few recent examples include papuamides A−D isolated from the Papua New Guinea sponges *Theonella mirabilis* and *Theonella swinhoei*,[3a] homophymine A obtained from New Caledonian specimens of *Homophymia* sp.,[3b] and mirabamides A−D[3c] and celebeside A[3d] isolated by our group from respective collections of *Siliquariaspongia* from Chuuk and Indonesia. As a result of our work on HIV entry inhibitors, here we describe the structure elucidation, biological activity, and taxonomic alignments of three sets of peptides that co-occur within deep-water specimens of *Theonella* sponges from Palau. These include collections of

(1) Fox, J. L. *Nat. Biotechnol.* **2007**, *25*, 1395.
(2) Hauber, I.; Bevec, D.; Heukeshoven, J.; Kratzer, F.; Horn, F.; Choidas, A.; Harrer, T.; Hauber, J. *J. Clin. Invest.* **2005**, *115*, 76.
(3) (a) Ford, P. W.; Gustafson, K. R.; McKee, T. C.; Shigematsu, N.; Maurizi, L. K.; Pannell, L. K.; Williams, D. E.; Dillip de Silva, E.; Lassota, P.; Allen, T. M.; Van Soest, R.; Andersen, R. J.; Boyd, M. R. *J. Am. Chem. Soc.* **1999**, *121*, 5899. (b) Zampella, A.; Sepe, V.; Luciano, P.; Bellota, F.; Monti, M. C.; D'Auria, M. V.; Jepsen, T.; Petek, S.; Adeline, M. -T.; Leprevote, O.; Aubertin, A.-M.; Bebitus, C.; Poupat, C.; Ahond, A. *J. Org. Chem.* **2008**, *73*, 5319. (c) Plaza, A.; Gustchina, E.; Baker, H. L.; Kelly, M.; Bewley, C. A. *J. Nat. Prod.* **2007**, *70*, 1753. (d) Plaza, A.; Bifulco, G.; Keffer, J. L.; Lloyd, J. R.; Baker, H. L.; Bewley, C. A. *J. Org. Chem.* **2009**, *74*, 504.

Published on Web 04/19/2010 DOI: 10.1021/jo100076g

Theonella cupola, *T. swinhoei* subspecies *verrucosa* Wilson (1925), and *T. swinhoei* subspecies *swinhoei* Gray (1869), the aqueous extracts of which inhibited HIV-1 infection, displayed antifungal activity against *Candida albicans*, or both. In addition to the biological profiles, the peptide distribution within these samples was ascertained by LC−MS analyses of the aqueous extracts, all of which yielded comparable chromatograms containing two marked regions with at least three different classes of peptides present in each. Subsequent structural studies led to the isolation of a new sulfated cyclic depsipeptide, termed mutremdamide A (**1**), three new linear peptides termed koshikamides C−E (**2**−**4**), and three new cyclic depsipeptides termed koshikamides F−H (**5**−**7**) together with the known peptides koshikamide B[4] (**8**) and theonellamide A.[5] Their structures were determined from NMR and HR-MS and MS-MS data and absolute configurations by Marfey's derivatization,[6] chiral HPLC, and the combined analysis of homonuclear (H−H) and heteronuclear (C−H) $^{2,3}J$ couplings and NOEs. Configurations of new amino acid residues were confirmed independently using quantum mechanical calculations.

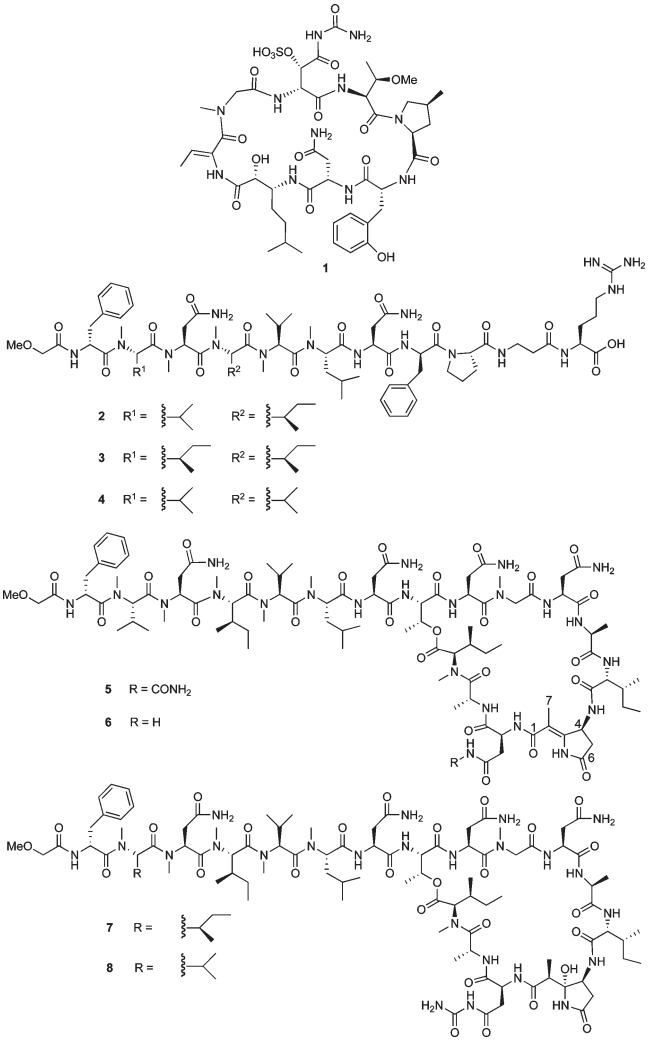

Results and Discussion

The crude aqueous extract of a deep-water specimen of *T. swinhoei* subspecies *swinhoei* Gray, 1869 (voucher specimen G329993, collection PA-08−05) was partitioned between *n*-BuOH and H_2O and the organic layer evaporated and separated by RP-HPLC (C12 column) to yield compounds **1**−**8**. The HR-CDESI-MS (corona discharge electrospray ionization) of mutremdamide A (**1**) showed a major ion peak at *m*/*z* 1068.4294 $[M + H]^+$ corresponding to a molecular formula of $C_{41}H_{65}N_{11}O_{18}S$. The presence of a sulfate group was indicated by a fragment ion peak at *m*/*z* 988.4804 $[M + H - SO_3]^+$ in the HR-ESI-MS and by IR bands at 1245 and 1086 cm^{-1}. The ^1H NMR spectrum of **1** in DMSO-d_6 showed signals ascribable to exchangeable NH protons from δ 6.00 to 9.02 and a signal corresponding to a methyl amide at δ 2.71 (3H, s), suggesting a peptidic structure for **1**. Additionally, a downfield pair of doublets at δ 7.16 (1H, d, J =7.3 Hz) and 6.88 (1H, d, J =7.8 Hz) together with a downfield pair of triplets at δ 7.11 (1H, t, J =7.8 Hz) and 6.80 (1H, t, J =7.3 Hz) indicated the presence of an *ortho*-substituted phenyl ring.

A detailed analysis of the 2D NMR data obtained from HSQC, HMBC, 2D-HOHAHA, and DQF-COSY experiments established the presence of the unusual amino acids 3-amino-2-hydroxy-6-methylheptanoic acid (Ahmha), 2-amino-but-2-enoic acid (Aba), *O*-methylthreonine (*O*MeThr), and 4-methylproline (4-Mep), along with one *N*-methylglycine and one asparagine residue. The presence of an *o*-tyrosine (*o*-Tyr) residue was indicated from the 2D NMR data. In particular, diagnostic HMBC correlations (see Table 1) from the α-methine proton at δ 4.12 (H-$2_{o\text{-Tyr}}$) to the carbon resonances at δ 170.7 (C-$1_{o\text{-Tyr}}$) and 124.1 (C-$1'_{o\text{-Tyr}}$) and from the β-methylene protons at δ 2.94 and 2.86 (H-$3_{o\text{-Tyr}}$) to the carbon resonances at δ 170.7, 124.1, 154.5 (C-$2'_{o\text{-Tyr}}$), and 130.3 (C-$6'_{o\text{-Tyr}}$) along with COSY correlations between the aromatic protons at δ 7.16 (H-$6'_{o\text{-Tyr}}$), 6.80 (H-$5'_{o\text{-Tyr}}$), 7.11 (H-$4'_{o\text{-Tyr}}$), and 6.88 (H-$3'_{o\text{-Tyr}}$) established the structure of this residue as the rare 2-amino-3-(2′-hydroxyphenyl)propanoic acid (*o*-Tyr).

The remaining spin system corresponded to a β-hydroxyasparagine (β-OHAsn) unit. However this residue also bore a sole downfield NH-4 proton at δ_H 8.88 (1H, s) that suggested substitution of the N^{δ} atom. Although no HMBC correlations were observed for this exchangeable proton, correlations with an unassigned pair of NH_2 protons at δ 7.50 (1H, br s) and 7.30 (1H, br s) were observed in the ROESY and HOHAHA spectra. Together with an unassigned quaternary carbon signal at δ_c 152.7 and loss of 59 Da in the MS/MS spectrum, these data supported addition of a carbamoyl moiety[7] linked to the δ-amide of β-OHAsn. Finally sulfation of the β-hydroxyl group was apparent from the downfield chemical shifts of the oxymethine (δ_H 4.60, δ_C 74.9). This appears to be the first example where a β-OHAsn residue is further modified by an N^{δ}-carbamoyl moiety and *O*-sulfation (N^{δ}-c-β-OSO_3Asn).

The complete cyclic amino acid sequence of mutremdamide A (**1**) was established from HMBC and ROESY spectra in a straightforward manner as all sequential long-range couplings and ROEs between α- and/or NH protons and neighboring carbonyls were observed. This

(4) Araki, T.; Matsunaga, S.; Nakao, Y.; Furihata, K.; West, L.; Faulkner, D. J.; Fusetani, N. *J. Org. Chem.* **2008**, *73*, 7889.
(5) Matsunaga, S.; Fusetani, N. *J. Org. Chem.* **1995**, *60*, 1177.
(6) (a) Fujii, K.; Ikai, Y.; Oka, H.; Suzuki, M.; Harada, K.-I. *Anal. Chem.* **1997**, *69*, 5146. (b) Fujii, K.; Ikai, Y.; Mayumi, T.; Oka, H.; Suzuki, M.; Harada, K.-I. *Anal. Chem.* **1997**, *69*, 3346.
(7) Bui, H. T. N.; Jansen, R.; Pham, H. T. L.; Mundt, S. *J. Nat. Prod.* **2007**, *70*, 499.

TABLE 1. NMR Spectroscopic Data for Mutremdamide A (1) (DMSO-d_6)

	1			
	δ_C[a]	δ_H[b] (J in Hz)	HMBC[c]	ROESY[d]
		o-Tyr		
1	170.7			
2	56.4	4.12 m	1, 3, 1′	3b, 6′, NH_{Asn}, 2_{OMeThr}
3a	30.5	2.94 t (12.7)	1, 2, 1′, 2′, 6′	6′, OH
3b		2.86 dd (12.7, 3.2)	1, 2, 1′, 2′, 6′	2, 6′
1′	124.1			
2′	154.5			
3′	114.4	6.88 d (7.8)	3, 1′, 2′, 5′, 6′	6′, OH, $3b_{4\text{-MePro}}$, Me-$4_{4\text{-MePro}}$
4′	127.8	7.11 t (7.8)	1′, 2′, 3′, 5′, 6′	2, 3b
5′	119.7	6.80 t (7.3)	1′, 2′, 3′, 4′, 6′	OH
6′	130.3	7.16 d (7.3)	3, 2′, 3′, 4′	2, 3b
NH		7.20 d (7.0)	2, 3, $1_{4\text{-MePro}}$	OH, $2_{4\text{-MePro}}$
OH		10.2 s	1′, 2′, 3′, 6′	3′, 5′ NH, 3a, $3b_{4MePro}$, $5b_{4\text{-MePro}}$, Me-$4_{4\text{-MePro}}$
		Asn		
1	170.4			
2	47.9	4.70 br s	1, 3, 4, $1_{o\text{-Tyr}}$	3a, 3b, 3_{Ahmha}, NH_{Ahmha}
3a	36.8	3.14 d (16.2)	2, 4	2
3b		2.42 d (16.2)	1, 2, 4	2, NH, NH-4
4		172.5		
NH_2-4		7.85, 6.52 br s	4	2, OMe$_{OMeThr}$
NH		7.18 d (7.8)	$1_{o\text{-Tyr}}$	3b, $1_{O\text{-Tyr}}$, OMe$_{OMeThr}$
		Ahmha		
1	169.8			
2	72.6	4.14 br s	1, 3, 4	3, NH, NH_{Aba}
3	51.8	4.00 d (1.5)	2, 4, 5, 1_{Asn}	2, 3, 4, 5, Me-6, NH, 2_{Asn}
4	24.0	1.40, 1.16 m	2, 3, 5, 6	3, NH, OH-2
5	34.2	1.15, 0.95 m	3, 4, 6, 7, Me-6	3, 6, 7, Me-6
6	27.0	1.41 m	5, 7, Me-6	5
7	21.7	0.772 d (6.2)	5, 6, Me-6	5
Me-6	22.3	0.775 d (6.2)	5, 6, 7	3, 5
NH		6.38 d (9.1)	3, 4, 1_{Asn}	2, 3, 4, OH-2, 2_{Asn}
OH-2		4.82 br s	1, 2	4, NH, NH_{Aba}, H-$2_{4\text{-MePro}}$
		Aba		
1	167.3			
2	132.0			
3	126.3	5.77 m	1, 2, 3	NMe$_{Aba}$
4	12.0	1.55 d (6.8)	1, 2, 3, 1_{Ahmha}	NH
NH		8.64 s	1, 2, 3, 1_{Ahmha}	4, 2_{Ahmha}, OH-2_{Ahmha}, 2_{Gly}
		*N*MeGly		
1	167.1			
2	51.4	4.21, 3.31 d (18.7)	1, *N*Me	*N*Me, NH_{Aba}, $2_{c\text{-}\beta\text{-OSO3Asn}}$, $NH_{c\text{-}\beta\text{-OSO3Asn}}$
*N*Me	34.4	2.71 s	2, 1_{Aba}	2, 3_{Aba}
		N^{δ}-c-β-OSO_3Asn		
1	167.6			
2	52.9	5.05 t (6.6)	1, 3, 4, $1_{N\text{MeGly}}$	NH-4, NH_{OMeThr}, $2_{N\text{meGly}}$
3	74.9	4.60 d (7.1)	1, 2, 4	NH-4, NH
4	170.7			
NH-4		8.88 s	4	2, 3, $CONH_2$, NH, $4_{O\text{meThr}}$
NH		7.16 d (7.4)	2, $1_{N\text{MeGly}}$	3, NH-4, $2_{N\text{meGly}}$
$CONH_2$	152.7	7.50, 7.30 br s		NH-4, $4_{O\text{meThr}}$
		*O*MeThr		
1	170.9			
2	55.3	4.92 br s	1, 3, $1_{c\text{-}\beta\text{-OSO3Asn}}$	4, NH, $2_{4\text{-MePro}}$, $5a_{4\text{-MePro}}$
3	72.9	4.16 m	2	OMe, $5b_{4\text{-MePro}}$
4	14.3	1.23 d (5.8)	2, 3	2, NH-$4_{c\text{-}\beta\text{-OSO3Asn}}$, c-$NH_{2c\text{-}\beta\text{-OSO3Asn}}$
OMe	54.5	3.27 s	3	3, NH_{Asn}, NH_2-4_{Asn}
NH		9.02 (9.2)	$1_{N\delta\text{-c-}\beta\text{-OSO3Asn}}$	2, 4, OMe, $2_{c\text{-}\beta\text{-OSO3Asn}}$
		4-MePro		
1	170.8			
2	63.2	3.90 dd (11.0, 6.7)	1, 3	3b, 4, 2_{OMeThr}, $NH_{O\text{-Tyr}}$
3	36.1	2.10, 0.72 m	1, 2, 4, 5, Me-4	2, 5b, $NH_{o\text{-Tyr}}$
4	33.2	2.25 m	3, 5 Me-4	2, 5a, Me-4
5a	52.8	4.11 dd (10.8, 6.9)	3, 4, 1_{OMeThr}	2_{OMeThr}
5b		3.41 t (10.8)	4, Me-4	3, Me-4, 3_{OMeThr}
Me-4	15.7	1.05	3, 4, 5	

[a]Recorded at 125 MHz; referenced to residual DMSO-d_6 at δ 39.51 ppm. [b]Recorded at 500 MHz; referenced to residual DMSO-d_6 at δ 2.50 ppm. [c]Proton showing HMBC correlation to indicated carbon. [d]Proton showing ROESY correlation to indicated proton.

sequence was consistent with the fragmentation pattern obtained from QTOF-MS/MS experiments. Fragmentation of the ion at m/z 987 $[M + H - SO_3H]^+$ displayed fragment ions at m/z 929 $[M + H - SO_3H\text{-}NHCONH_2]^+$,

m/z 617 [M + H − SO_3H-NHCONH$_2$-Ahmha-Aba-*N*-MeGly]$^+$, m/z 389 [M + H − SO_3H-NHCONH$_2$-Ahmha-Aba-*N*MeGly-Asn-*O*MeThr]$^+$, and m/z 275 [M + H − SO_3H-NHCONH$_2$-Asn-Ahmha-Aba-*N*MeGly-Asn-*O*MeThr]$^+$ corroborating the sequence obtained by NMR.

At this point, it was evident that the amino acid sequence of mutremdamide A was related to that of perthamide B recently isolated from an Australian specimen of *Theonella* sp.[8] These two peptides differ by three residues, where perthamide B contains *m*-bromotyrosine, *β*-hydroxyasparagine, and 3-amino-2-hydroxy-6-methyloctanoic acid residues versus mutremdamide A that contains *o*-Tyr, N^{δ}-c-*β*-OSO_3Asn, and Ahmha residues.

The configurations of the chiral centers in **1** were solved using a combination of techniques. A strong NOE between the NH (*δ* 8.64) and vinyl methyl (*δ* 1.55) signals established a *Z* geometry for the Aba residue. The absolute configurations of *erythro*-D-N^{δ}-c-*β*-OSO_3Asn, L-*O*MeThr, and D-*o*-Tyr were assigned by chromatographic (UV and TLC) comparison of the L- and D-FDLA (1-fluoro-2,4-dinitrophenyl-5-L/D-leucinamide) derivatives of the acid hydrosylate of **1** with L/D-FDLA derivatives of respective amino acid standards (advanced Marfey's method).[6] The absolute configuration of C-2 in the 4-MePro residue was also determined by the advanced Marfey's method. In particular, reconstructed ion chromatograms (m/z 422, [M − H]$^-$) of L- and D-FDLA derivatized hydrosylates of **1** showed peaks eluting at 25.1 and 28.1 min, respectively. Because L derivatives of 4-MePro elute before their D derivatives,[9] the configuration of C-2 was assigned as L. Analysis of the $^3J_{H-H}$ coupling constants obtained from ^{1}H NMR, TOCSY, and E.COSY[10] experiments along with ROESY correlations allowed us to determine the orientation of the methyl group at C-4. Large $^3J_{H-H}$ coupling constants between H-2$_{4\text{-MePro}}$ and H-3a$_{4\text{-MePro}}$ and between H-4$_{4\text{-MePro}}$ and H-5a$_{4\text{-MePro}}$ (11.0 and 10.8 Hz, respectively) suggested *trans* diaxial relationships for each of these proton pairs. Moreover, correlations from H-2$_{4\text{-MePro}}$ to H-4$_{4\text{-MePro}}$ and from H-3a$_{4\text{-MePro}}$ to H-5a$_{4\text{-MePro}}$ were observed in the ROESY spectrum. Together these data revealed a *cis* arrangement between H-4$_{4\text{-MePro}}$ and H-2$_{4\text{-MePro}}$ (Figure 1A).

We independently assessed the relative stereochemistry of the 4-MePro residue by performing quantum mechanical calculations of its $^3J_{H-H}$ coupling constants. Two diastereoisomeric models of 4-MePro containing either a *cis* or *trans* relationship between H-2$_{4\text{-MePro}}$ and H-4$_{4\text{-MePro}}$ were prepared, and a preliminary conformational search was performed using molecular dynamics calculations (5 ns time steps) at several temperatures. For both the *cis* and *trans* models, two main sets of conformers were observed where the major and minor ones differed by 3.25 and 7.82 kJ, respectively. Force field geometries were further optimized at the density functional theory (DFT) level, and the coupling constants for the protons of optimized geometries were calculated using the mPW1PW91 DFT functional and the 6-31G(d,p) basis set. The results are shown in Table 2 where

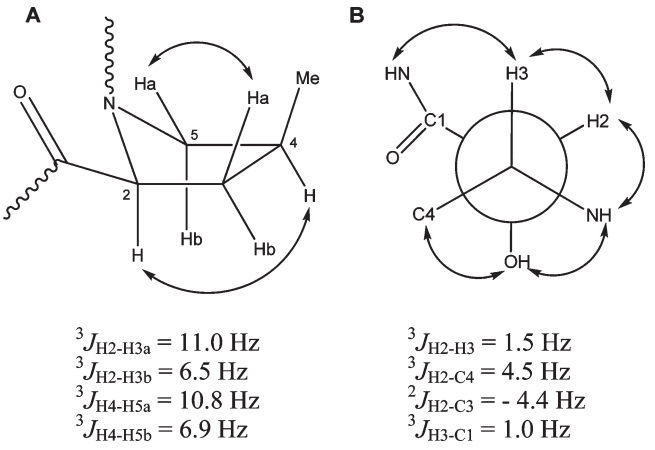

FIGURE 1. (A) Key ROESY correlations and selected $^3J_{H-H}$ values of the 4-MePro residue in **1**. (B) Newman projection, ROESY correlations and $^{2,3}J$ coupling constants used to determine the configuration of C-2/C-3 in the Ahmha residue in **1**.

TABLE 2. Calculated and Experimental $^3J_{H-H}$ Values (Hz) of the 4-MePro Portion in 1 for the Two Conformational Arrangements Belonging to *Cis* and *Trans* Configurations

	calculated[a]				
	cis major	*cis* minor	*trans* major	*trans* minor	experimental[b]
$^3J_{H2-H3a}$	8.6	9.3	7.8	8.7	11.0
$^3J_{H2-H3b}$	6.9	0.5	0.3	6.8	6.5
$^3J_{H4-H5a}$	9.6	7.0	9.3	5.2	10.8
$^3J_{H4-H5b}$	6.6	0.4	7.6	0.3	6.9
TAD	***4.3***	*18.0*	*11.6*	*14.8*	

[a]MPW1PW91/6-31G(d,p) calculated *J* values (Hz). [b]Experimental values obtained from ^{1}H NMR, TOCSY, and E.COSY correlations. Total absolute deviation (TAD) values calculated from the equation ($\Sigma|J_{calc} - J_{exp}|$). Stereoisomer displaying lowest TAD value appears in bold.

the calculated and experimentally determined values are compared. The total absolute deviation (TAD) values ($\Sigma|J_{calc} - J_{exp}|$), shown in italics, unambiguously demonstrate that only the calculated *J* values corresponding to the major conformer with a *cis* configuration are in agreement with the experimental $^3J_{H-H}$ coupling constants, thus corroborating our NMR analysis. Having established the absolute configuration of C-2$_{4\text{-MePro}}$ as *S* by the advanced Marfey's derivatization, the absolute configuration at C-4$_{4\text{-MePro}}$ was assigned as *S*.

The relative configuration of the amino group at C-3 and the hydroxyl group attached to C-2 in the Ahmha residue was established by using a combination of *J*-based configurational analysis,[11] quantum mechanical calculations of the homonuclear and heteronuclear *J*-coupling values, and ROESY correlations. The heteronuclear coupling constants were accurately measured from *J*-resolved HMBC[12] and HSQMBC[13] experiments. The gauche orientation between H-2$_{Ahmha}$ and H-3$_{Ahmha}$ was deduced from their small $^3J_{H-H}$ coupling constant (1.5 Hz). $^3J_{C-H}$ values of 4.5 Hz for H-2$_{Ahmha}$/C-4$_{Ahmha}$ and of 1.0 Hz for H-3$_{Ahmha}$/C1$_{Ahmha}$

(8) Gulavita, N. K.; Pomponi, S. A.; Wright, A. E.; Yarwood, D.; Sils, M. A. *Tetrahedron Lett*. **1994**, *35*, 6815.
(9) Murphy, A. C.; Mitova, M. I.; Blunt, J. W.; Munro, M. H. G. *J. Nat. Prod*. **2008**, *71*, 806–809.
(10) Griesinger, C.; Sorensen, O. W.; Ernst, R. R. *J. Magn. Reson*. **1987**, *75*, 474.
(11) Matsumori, N.; Kaneno, D.; Murata, M.; Nakamura, H.; Tachibana, K. *J. Org. Chem*. **1999**, *64*, 866.
(12) Meissner, A.; Soerensen, O. W. *Magn. Reson. Chem*. **2001**, *39*, 49.
(13) (a) Marquez, B. L.; Gerwick, W. H.; Williamson, R. T. *Magn. Reson. Chem*. **2001**, *39*, 499. (b) Williamson, R. T.; Marquez, B. L.; Gerwick, W. H.; Kover, K. E. *Magn. Reson. Chem*. **2000**, *38*, 265.

TABLE 3. Calculated and Experimental *J* Values (Hz) of the Ahmha Residue in 1

	calculated[a]						
	threo			*erythro*			
	anti	*gauche* -	*gauche* +	*anti*	*gauche* -	*gauche* +	experimental[b]
$^3J_{H2-H3}$	8.5	5.3	1.4	7.6	3.3	3.0	1.5
$^3J_{H3-C1}$	1.9	6.2	1.0	0.5	6.6	0.5	1.0
$^3J_{H2-C4}$	1.3	4.3	1.8	4.2	1.0	3.9	4.5
$^2J_{H2-C3}$	−1.0	−0.9	2.5	−2.8	1.1	−3.0	−4.4
TAD	*14.5*	*12.6*	*9.8*	*8.5*	*16.3*	***4.0***	

[a]MPW1PW91/6-31G(d,p) calculated *J* values. [b]Experimental values obtained from *J*-resolved HMBC and HSQMBC spectra. Total absolute deviation (TAD) values calculated from the equation ($\Sigma|J_{calc} - J_{exp}|$). Steroisomer displaying lowest TAD value appears in bold.

indicated an anti orientation between H-2$_{Ahmha}$ and C-4$_{Ahmha}$ and a gauche orientation between H-3$_{Ahmha}$ and C-1$_{Ahmha}$, while a $^2J_{C-H}$ value of −4.4 Hz for H-2$_{Ahmha}$/C-3$_{Ahmha}$ suggested a gauche orientation for H-2$_{Ahmha}$ and the amide group in C-3$_{Ahmha}$. On the basis of these data, the relative configuration between stereocenters C-2 and C-3 in the Ahmha residue was assigned as *erythro* (Figure 1B). We note that although the value for $^2J_{C-H}$ between H-2 and C-3 obtained from the *J*-resolved HMBC spectrum has an absolute value of 4.4 Hz, this coupling constant is negative since values for $^2J_{C-H}$ range from −6 to +2 Hz.[11]

Recently, we have shown the utility of using a combined NMR−quantum mechanical calculations approach to determine the configuration of chiral centers within a macrocycle and in cases where the calculated $^{2,3}J_{C-H}$ cannot be qualitatively classified as "large" or "small".[2] This approach is based on the quantitative comparison of the experimental and calculated $^3J_{H-H}$ and $^{2,3}J_{C-H}$ values.[14] We applied this approach here to calculate the relevant *J* values of the Ahmha residue in **1** at the DFT MPW1PW91/6-31G(d,p) level (see the Experimental Section). The results are shown in Table 3, where the calculated values for the six possible conformers (three *threo* and three *erythro* arrangements) for the C2−C3 stereocenter pair are compared to the experimental values obtained by NMR. The *erythro* gauche + arrangement displays the lowest TAD value, which is in full agreement with the *J*-based analysis presented above. Finally, NOEs between H-4$_{Ahmha}$/OH-2$_{Ahmha}$, OH-2$_{Ahmha}$/NH$_{Ahmha}$, NH$_{Ahmha}$/H-2$_{Ahmha}$, H-2$_{Ahmha}$/H-3$_{Ahmha}$, and H-3$_{Ahmha}$/NH$_{Aba}$ (Table 1) further supported these results corroborating the *erythro* configuration between the C-2 hydroxyl and C-3 amide (see Figure 1B).

With the relative configuration of C-2/C-3 in hand, we were able to establish the absolute configuration at C-3 using advanced Marfey's analysis. The L- and D-FDLA derivatives of Ahmha were detected at retention times of 34.4 and 28.0 min on the reconstructed ion chromatogram for *m*/*z* 468 $[M - H]^-$. As shown by Fuji et al. for aliphatic β-amino acids,[6,15] the L-FDLA derivative of 3*S*-Ahmha should elute before the same derivative of 3*R*-Ahmha because an FDLA derivative bearing a *cis*-type arrangement is expected to be more hydrophobic than one bearing a *trans*-type arrangement and the isopentyl side chain of Ahmha is more hydrophobic than the hydroxy carboxylic acid moiety. On the basis of these results, the absolute configuration of C-3 was assigned as *R*, giving the absolute configuration of Ahmha as (2*R*, 3*R*)-3-amino-2-hydroxy-6-methylheptanoic acid.

During the preparation of this manuscript, Zampella and co-workers reported the structures of perthamides C and D, isolated from a specimen of *T. swinhoei* collected in the Solomon Islands.[16] The amino acid sequences of perthamides C and D are similar to **1**, but several key differences in composition and configuration exist. First, mutremdamide A differs from perthamide C by the mutual presence of sulfation and carbamoylation of the β-OH and N^δ-amide groups of β-OHAsn, respectively. Surprisingly, a careful comparison of the ^{1}H and ^{13}C NMR data for mutremdamide A in CD_3OD (see Table S1, Supporting Information) and perthamide C in the same solvent failed to show major differences in chemical shifts, even for the β position of the β-OHAsn residue. The similarities in these downfield values (perthamide C: δ_H 4.94, δ_C 77.8; **1**: δ_H 4.91, δ_C 77.6) together with the nontrivial MS approach required to detect sulfated mutremdamide A led us to speculate that perthamide C may also contain a β-*O*-(SO_3)H moiety. In our experience, we were unable to detect the molecular ion of **1** using standard ESI conditions that we have described for other complex peptides.[3c,d] Instead, detection could only be accomplished by employing corona discharge electrospray ionization (CDESI) conditions.[17] Under CDESI, the ESI capillary is held at 5 KV allowing a large amount of corona discharge to be observed at the exit tip of the capillary. Under these conditions, we can detect sulfates and phosphates that normally adhere to the stainless steel of the electrospray capillary and are otherwise not detectable. During CDESI, the stainless steel surface of the capillary is electrochemically modified, possibly removing the binding sites responsible for suppression of compounds such as phosphates and sulfates. It is also interesting to note the unusual downfield signal of perthamide C assigned to NH_2-4 of β-OHAsn (δ_H 9.40), the equivalent of which we assign to the N^δ-carbamoyl atom. In consideration of these data together with the similar δ_C values for the C-4$_{\beta-OHAsn}$ atoms (δ 172.0 vs 172.2), it is possible that perthamide C also bears substitution on its N^δ atom.

Another key difference between mutremdamide A and perthamide C is the relative configuration for the C-2 hydroxyl and C-3 amino groups in the Ahmha residue. For perthamide C, the relative configuration at C-2/C-3 was assigned as *threo* on the basis of *J*-couplings, whereas mutremdamide A shows an *erythro* configuration assigned on the basis of three complementary and converging data sets. Although major differences in homonuclear and heteronuclear $^{2,3}J$ couplings are reported, where respective $^3J_{H2-C4}$ values of 1.4 and 4.5 Hz and respective $^2J_{H2-C3}$ values of −1.8 Hz and −4.4 Hz are reported for perthamide C versus **1**, their ^{1}H and ^{13}C chemical shifts are nearly identical. It will be interesting to compare relative configurations and chemical shift values for future peptides of this class.

(14) (a) Bifulco, G.; Bassarello, C.; Riccio, R.; Gomez- Paloma, L. *Org. Lett.* **2004**, *6*, 1025. (b) Bifulco, G.; Dambruoso, P.; Gomez-Paloma, L.; Riccio, R. *Chem. Rev.* **2007**, *107*, 3744.

(15) Fujii, K.; Sinoven, K.; Kashiwagi, T.; Hirayama, K.; Harada, K.-I. *J. Org. Chem.* **1999**, *64*, 5777.

(16) Festa, C.; De marino, S.; Sepe, V.; Monti, M. C.; Luciano, P.; D'Auria, M. V.; Debitus, C.; Bucci, M.; Velleco, V.; Zampella, A. *Tetrahedron* **2009**, *65*, 10424.

(17) Lloyd, J. R.; Hess, S. *J. Am. Soc. Mass. Spectrom.* **2003**, *11*, 1988.

The second suite of compounds in this extract was composed of the linear koshikamides C−E (**2**−**4**), with koshikamide C being the most abundant of this group. The molecular formula of koshikamide C (**2**) was shown to be $C_{70}H_{110}N_{16}O_{16}$ by HR-ESI-MS (*m*/*z* 1431.8330 $[M + H]^+$) and NMR spectral data (Table 4). 2D NMR data established the presence of two phenylalanine residues, two *N*-methylvalines, one *N*-methylasparagine, one *N*-methylisoleucine, one *N*-methyleucine, one asparagine, one proline, one β-alanine, one arginine, and one 2-methoxyacetic acid (Maa) moiety. Moreover, two sets of signals in a ratio of 3:2 were observed for Asn, Phe2, Pro, β-Ala, and Arg (see Table 4 and Table S2, Supporting Information) suggesting that the proline residue in koshikamide C (**2**) undergoes *cis*/*trans* isomerization resulting in the presence of two stable conformers. This was evident from the differential δ_C values for C_β and C_γ ($\Delta\delta_{\beta\gamma}$) of the two proline spin systems which allowed us to identify the major conformer as *trans* ($\delta_{H\text{-}\alpha}$ 4.14, $\delta_{C\text{-}\alpha}$ 59.6; $\Delta\delta_{\beta\gamma}$ =5.3) and the minor as *cis* ($\delta_{H\text{-}\alpha}$ 4.72, $\delta_{C\text{-}\alpha}$ 59.6; $\Delta\delta_{\beta\gamma}$ =9.9) (see Table 4 and Tables S2 and S3, Supporting Information).[18] HMBC correlations between α, NH, and *N*Me protons to carbonyl carbons of adjacent amino acids, and NOEs, assigned from ROESY and HSQC-ROESY[19] spectra, between α and sequential NH and *N*Me protons allowed us to assign two fragments in **2**: Maa-Phe1-*N*MeVal1-*N*MeAsn-*N*MeIle-*N*MeVal2-*N*MeLeu-Asn-Phe2 and Pro-βAla-Arg. Unambiguous connectivity between these two fragments was deduced from the ROESY spectrum. An ROE from H-4a_{Pro} (δ 3.54) to H-1$_{Phe2}$ (δ 4.63) established the complete sequence for the *trans* conformer of **2** (see Table 4) and from H-1a_{Pro*} (δ 4.72) to H-1$_{Phe2*}$ (δ 4.28) for the *cis* conformer (see Table S2, Supporting Information). The peptide sequence of **2** was also corroborated by ESI-MS/MS analysis. Fragmentation of the major ion peak at *m*/*z* 1432 $[M + H]^+$ yielded ion peaks at *m*/*z* 1212 $[M + H -$ Maa-Phe$]^+$, *m*/*z* 1099 $[M + H -$ Maa-Phe-*N*MeVal$]^+$, *m*/*z* 970 $[M + H -$ Maa-Phe-*N*MeVal-*N*MeAsn$]^+$, *m*/*z* 844 $[M + H -$ Maa-Phe-*N*MeVal-*N*MeAsn-*N*MeIle$]^+$, *m*/*z* 731 $[M + H -$ Maa-Phe-*N*MeVal-*N*MeAsn-*N*MeIle-*N*MeVal$]^+$, *m*/*z* 602 $[M + H -$ Maa-Phe-*N*MeVal-*N*MeAsn-*N*MeIle-*N*MeVal-*N*MeLeu$]^+$, and *m*/*z* 489 $[M + H -$ Maa-Phe-*N*MeVal-*N*MeAsn-*N*MeIle-*N*MeVal-*N*MeLeu-Asn$]^+$, in full agreement with our NMR results.

The absolute configuration of koshikamide C (**2**) was determined using the same methods described above for mutremdamide A (**1**) and established an L configuration for both *N*MeVal residues, *N*MeAsn, Asn, *N*MeLeu, and Pro, while the two Phe residues were shown to be D. In similar fashion, comparison of L/D-FDLA derivatives of authentic standards to that of the acid hydrolysate showed the *N*MeIle residues to be L-*N*Me-*allo*-Ile.

HR-ESI-MS data for koshikamides D (**3**) and E (**4**) indicated molecular formulas of $C_{71}H_{112}N_{16}O_{16}$ (*m*/*z* 1445.8514 $[M + H]^+$) and $C_{69}H_{108}N_{16}O_{16}$ (*m*/*z* 1417.8177 $[M + H]^+$), respectively. Relative to koshikamide C, these molecular weights were 14 mass units higher for koshikamide D and 14 mass units lower for koshikamide E. Analysis of their NMR and MS/MS data indicated that **3** and **4** possess similar amino acid sequences to that of **2**, with the differences traced to substitution of *N*MeVal1 in **2** by *N*MeIle in **3**, and of *N*Me-*allo*-Ile in **2** by *N*MeVal2 in **4**. Again, configurations of L-*N*Me-*allo*-Ile in **3** and L-*N*MeVal in **4** were established by LC-MS analysis of their respective L-FDLA and D-FDLA-derivatized hydrolysates in comparison to their respective amino acid standards.

Evident from the LC-MS total ion chromatograms (TIC), the aqueous extracts of two of the three *Theonella* samples also included a set of compounds with considerably larger masses and increased hydrophobicity compared to compounds **1**-**4**. The HR-ESI-MS of koshikamide F (**5**) showed a major ion peak at *m*/*z* 2032.0912 $[M - H]^-$ corresponding to a molecular formula of $C_{93}H_{148}N_{24}O_{27}$. Although considerable overlap existed in the ^{1}H NMR spectrum of **5**, it nonetheless exhibited signals characteristic of a peptide including NH resonances between δ 7.62 and 10.50 and four *N*-methyl amides at δ 2.89 (3H, s), 2.80 (3H, s), and 2.76 (6H, s) (see Table 4). Moreover, its UV spectrum showed absorbance at 270 nm suggesting the presence of a simple conjugated chromophore. The HSQC spectrum of **5** clearly showed that the 18 proton signals at δ 3.66−5.67 were correlated to 17 carbons at δ 45.2−63.6 (16 α-methines and one α-methylene), revealing the occurrence of seventeen amino acid residues. This evidence in combination with DQF-COSY, 2D-HOHAHA, HSQC-TOCSY, HSQC, and HMBC experiments allowed us to identify spin systems corresponding to the following residues: 2-methoxyacetic acid, phenylalanine, threonine, isoleucine, *N*-methylglycine, *N*-methyleucine, *N*-methylasparagine, two alanines, two *N*-methylvalines, two *N*-methylisoleucines, three asparagines, and the unusual N^δ-carbamoylasparagine. The presence of an atypical spin system comprising an amide proton at δ 8.33 and methine (δ_H 5.12, δ_C 45.2) and methylene (δ_H 2.88, 1.96, δ_C 36.5) signals was apparent from HSQC-TOCSY and COSY data. HMBC correlations from the methylene proton at δ 2.88 (H-5a_{Apdp}) to the carbonyl at δ 175.0 (C-6$_{Apdp}$) and from the amide proton at δ 10.5 (NH-6$_{Apdp}$) to the carbon resonances at δ 36.5 (C-5$_{Apdp}$) and 45.2 (C-4$_{Apdp}$) showed these signals to belong to a pyrrolidone ring. Finally, HMBC correlations from the methyl olefinic proton at δ 1.58 (Me-7$_{Apdp}$) to the carbon resonances at δ 168.4 (C-1$_{Apdp}$), 148.6 (C-2$_{Apdp}$), and 99.8 (C-3$_{Apdp}$), and ROESY correlations to protons at δ 5.12 (H-4$_{Apdp}$), 2.88 (H-5a_{Apdp}), 8.53 (NH-4$_{Apdp}$), and 10.50 (NH-6$_{Apdp}$) secured the structure of this residue as 2-(3-amino-5-oxopyrrolidin-2-ylidene)propanoic acid (Apdp). The *Z* geometry of the C2$_{Apdp}$−C3$_{Apdp}$ double bond was assigned from ROESY correlations between Me-7$_{Apdp}$ and H-4$_{Apdp}$ and NH-4$_{Apdp}$ (see Table 4 and Figure 2).

With the amino acid composition of **5** in hand, it was clear that koshikamide F was nearly identical to koshikamide B (**8**),[4] a complex peptide isolated from specimens of *Theonella* sp. from Japan and Palau and recently published by Matsunaga and co-workers. The key difference between these two peptides occurs in the pyrrolidinone-containing amino acids, where koshikamide B contains the hydroxylated AHPP residue and koshikamide F contains the new unit (*Z*)-2-(3-amino-5-oxopyrrolidin-2-ylidene)propanoic acid (see Figure 2). The QTOF-MS spectrum of **5** showed fragment ions at *m*/*z* 1701 $[M + H -$ Maa-Phe-*N*MeVal1$]^+$, *m*/*z* 1573 $[M + H -$ Maa-Phe-*N*MeVal1-*N*MeAsn$]^+$, *m*/*z* 1446 $[M + H -$ Maa-Phe-*N*MeVal1-*N*MeAsn-*N*MeIle1$]^+$,

(18) Siemion, I. Z.; Wieland, T.; Pook, K. H. *Angew. Chem., Int. Ed. Engl.* **1975**, *14*, 702.
(19) Bax, A.; Davis, D. G. *J. Magn. Reson.* **1985**, *63*, 207.

TABLE 4. NMR Spectroscopic Data for Koshikamide C (2) and F (5) (DMSO-d_6)

	2 (*trans* isomer)				**5**		
position	δ_C[a]	δ_H[b] (*J* in Hz)	ROESY[c]		δ_C[a]	δ_H[b] (*J* in Hz)	ROESY[c]
	2-methoxyacetic acid (Maa)				2-methoxyacetic acid (Maa)		
1	168.8			1	168.6		
2	70.7	3.75 s	OMe, NH_{Phe1}	2	70.7	3.75 s	OMe, NH, 2_{Phe}, NH_{Phe}
OMe	58.1	3.21 s	NH_{Phe1}, $2'_{Phe1}$, $3'_{Phe1}$	OMe	58.1	3.21 s	2, 2_{Phe}, $2'_{Phe}$ NH_{Phe}
	Phe1				Phe		
1	171.2			1	171.1		
2	49.9	4.93 m	3, 2′, NH, NMe_{NVal1}	2	50.0	4.93 m	3, 2′, NH, 2_{Maa}, OMe_{Maa}, $NMe_{NMeVal1}$
3a	36.4	3.02 dd (13.7, 5.9)	2, 2′, NH, $4_{NMeVal1}$	3a	36.4	3.00 dd (13.5, 5.8)	2, 2′, NH, $4_{NMeVal1}$
3b		2.91 m	2, 2′, NH, $4_{NMeVal1}$	3b		2.88 m	2, 2′, NH, $4_{NMeVal1}$
1′	137.1			1′	137.4		
2′, 6′	129.1	7.28[d]	2, 3, NH, OMe_{Maa}, $4_{NMeVal1}$	2′, 6′	128.9	7.28[d]	2, 3, NH, OMe_{Maa}
3′, 5′	127.8	7.26[d]	3, $4_{NMeVal1}$	3′, 5′	127.8	7.27[d]	3
4′	126.2	7.20[d]		4′	126.2	7.20[d]	
NH		8.03 d (7.9)	2, 3, 2_{Maa}, OMe_{Maa}	NH		8.04 d (8.6)	2, 3, 2_{Maa}, OMe_{Maa}
	*N*MeVal1				*N*MeVal1		
1	168.7			1	168.5		
2	58.0	4.91 d (10.6)	3, 4, 5, NMe_{NMeAsn}	2	57.9	4.90 d (10.6)	3, 4, 5, NMe_{NMeAsn}
3	26.4	2.17 m	2, 4, 5, *N*Me, NMe_{NMeAsn}	3	26.5	2.16 m	2, 4, 5, *N*Me, NMe_{NMeAsn}
4	17.6	0.59 d (6.5)	2, 3, 3_{Phe1}, $2'_{Phe1}$, $3'_{Phe1}$	4	17.4	0.58 d (6.5)	2, 3, 3_{Phe1}, $2'_{Phe}$, $3'_{Phe}$
5	19.4	0.79 d (6.5)	2, 3, *N*Me	5	19.3	0.79[d]	2, 3, *N*Me
*N*Me	29.5	2.89 s	3, 4, 2_{Phe1}	*N*Me	29.6	2.89 s	3, 4, 2_{Phe}
	*N*MeAsn				*N*MeAsn		
1	169.3			1	169.1		
2	49.7	5.67 dd (9.8, 3.7)	3, *N*Me, $NMe_{NMe\text{-}allo\text{-}Ile}$, $4_{NMeVal2}$	2	49.7	5.67 dd (10.0, 4.4)	3, *N*Me, $NMe_{NMe\text{-}allo\text{-}Ile}$, $4_{NMeVal2}$
3a	34.2	2.83[d]	2, NH_2-4	3a	34.3	2.82[d]	2, NH_2-4
3b		2.01 dd (15.2, 3.6)	2, NH_2-4	3b		2.01 dd (14.9, 3.8)	2, NH_2-4
4	171.0			4	170.8		
*N*Me	30.1	2.76 s	2, $2_{NMeVal1}$, $3_{NMeVal1}$	*N*Me	30.1	2.76 s	2, $2_{NMeVal1}$, $3_{NMeVal1}$
NH_2-4		7.33, 6.84 br s	3a	NH_2-4		7.34, 6.84 br s	3a
	*N*Me-*allo*-Ile				*N*Me-*allo*-Ile1		
1	169.0			1	169.0		
2	56.1	5.06 d (10.3)	3, 4, 5, 6, *N*Me, $NMe_{NMeVal2}$	2	55.9	5.05 d (10.7)	3, 4, 5, 6, *N*Me $NMe_{NMeVal2}$
3	32.2	2.08 m	2, 4, 5, 6, *N*Me	3	32.1	2.08 m	2, 4, 5, 6, *N*Me
4	25.2	1.23, 0.98 m	2, 3, 4	4	24.9	1.22, 0.95 m	2, 3, 4
5	10.7	0.81[d]	2, 3, *N*Me	5	10.4	0.80[d]	2, 3, *N*Me
6	13.4	0.65 d (6.5)	2, 3, *N*Me	6	13.0	0.65 d (6.5)	2, 3, *N*Me
*N*Me	29.1	2.80 s	2, 3, 5, 6, 2_{NMeAsn}	*N*Me	29.1	2.80 s	2, 3, 5, 6, 2_{NmeAsn}
	*N*MeVal2				*N*MeVal2		
1	170.0			1	169.9		
2	57.6	5.07 d (10.3)	3, 4, 5, *N*Me, NMe_{NMeLeu}	2	57.5	5.08 d (10.3)	3, 4, 5, *N*Me, NMe_{NMeLeu}
3	26.7	2.17 m	2, 4, 5	3	26.5	2.16 m	2, 4, 5
4	17.7	0.74 d (6.5)	2, 3, 2_{NMeAsn}	4	17.3	0.74 d (6.5)	2, 3, 2_{NMeAsn}
5	19.5	0.84[d]	2, 3	5	19.5	0.85[d]	2, 3
*N*Me	29.2	2.76 s	2, $2_{NMe\text{-}allo\text{-}Ile}$	*N*Me	29.1	2.76 s	2, $2_{NMe\text{-}allo\text{-}Ile}$
	*N*MeLeu				*N*MeLeu		
1	170.0			1	170.0		
2	53.2	5.11 dd (11.3, 3.8)	3, 4, 5, NH_{Asn}	2	53.1	5.12 m	3, 4, 5, NH_{Asn}
3	35.9	1.62, 1.45 m	2, 4, 5, 6, *N*Me	3	36.4	1.65, 1.48 m	2, 4, 5, 6, *N*Me
4	24.3	1.17 m	2, 3, 5, 6	4	24.3	1.19 m	2, 3, 5, 6
5	20.8	0.79[d]	2, 3	5	20.8	0.79[d]	2, 3
6	23.0	0.86[d]	2, 3	6	23.1	0.86[d]	2, 3
*N*Me	30.1	2.82 s	3, 4, 6, $2_{NMeVal2}$	*N*Me	30.0	2.85 s	3, 4, 6, $2_{NMeVal2}$
	Asn				Asn1		
1	170.5			1	170.2		
2	49.3	4.55 dd (14.0, 6.9)	3, NH, NH_{Phe2}	2	49.5	4.48 m	3, NH, NH_{Thr}
3	37.0	2.36 m	2, NH, NH_2-4	3	36.5	2.44 m	2, NH, NH_2-4
4	171.4			4	171.4		
NH_2-4		7.327, 6.94 br s	3	NH_2-4		7.27, 6.99 br s	3
NH		7.73 d (7.7)	2, 3, 2_{NMeLeu}, NMe_{NMeLue}	NH		7.72 br s	2, 3, 2_{NMeLeu}
	Phe2				Thr		
1	169.0			1	167.5		
2	52.0	4.63 dd (14.2, 7.0)	3, 2′, NH, 5_{Pro}	2	54.7	4.52 t (8.6)	4, NH_{Asn2}
3a	37.2	2.92[d]	2′, 6′	3	70.4	4.86 m	4
3b		2.81[d]	2′, 6′	4	15.8	0.93[d]	2, 3

TABLE 4. Continued

	2 (*trans* isomer)				**5**		
position	δ_C[a]	δ_H[b] (*J* in Hz)	ROESY[c]		δ_C[a]	δ_H[b] (*J* in Hz)	ROESY[c]
1′	137.0			NH		7.66[d]	2, 2_{Asn1}
2′, 6′	129.0	7.17 br d (7.5)	3a, 3b				
3′, 5′	128.8	7.21 m					
4′	121.3	7.25 m					
NH		8.09 d (8.6)	2, 3b, 2_{Asn}				
		Pro				Asn2	
1	171.1			1	171.7		
2	59.6	4.14 dd (8.4, 3.0)	3, $2'_{Phe2}$, $NH_{\beta\text{-Ala}}$	2	45.2	4.93 m	3, NH, NMe$_{NMeGly}$
3	28.9	1.85, 1.74 m	NH, 5a	3	36.7	2.64, 2.40 m	3, NH, NH_2-4
4	23.6	1.76, 1.63 m		4	169.4		
5a	46.2	3.54 br s	4, 5b, 2_{Asn}, $NH_{\beta\text{-Ala}}$	NH_2-4		7.60, 7.09 br s	3
5b		3.09[c] m	5a, 2_{Asn}, $2'_{Phe}$	NH		8.52 d (4.6)	2, 3, 2_{Thr}
		β-Ala				*N*MeGly	
1	170.4			1	170.0		
2	34.7	2.31 t (6.8)	3, NH, NH_{Arg}	2a	51.7	4.37 d (15.4)	
3	35.2	3.22 m		2b		3.66[d]	*N*Me
NH		7.59 m	2, 3, 2_{Pro}, $5a_{Pro}$	*N*Me	36.3	3.18 s	2b, 2_{Asn2}
		Arg				Asn3	
1	173.5			1	171.2		
2	51.1	4.20 m	3, 4, 5, NH	2	49.7	4.49 m	3, NH_{Ala1}, 4_{Apdp}, $NH_{c\text{-Asn}}$
3	28.0	1.73, 1.59 m	2, 5, NH-5, NH	3	36.0	2.42 m	NH, NH_2-4
4	24.9	1.49 m	2, 5, NH-5, NH	4	170.7		
5	40.0	3.09 m	2, 3, 4, NH-5	NH_2-4		7.35, 6.95 br s	3
NH-5		7.55 t (5.6)		NH		7.94	3, 4_{Apdp}, NH_{Apdp}, $NH_{c\text{-Asn}}$
6	156.6		3, 4, 5				
NH		8.18 d (7.7)	2, 3, 4, $2_{\beta\text{-Ala}}$				
						Ala1	
				1	172.1		
				2	48.5	4.16 m	3, NH_{Ile}
				3	16.8	1.21[d]	2, NH
				NH		7.79[d]	3, 2_{Asn3}
						Ile	
				1	169.1		
				2	56.9	3.99 t (7.1)	3, 4, 5, 6, NH-4_{Apdp}
				3	35.0	1.91 m	2, 4, 5
				4	23.9	1.35, 1.11 m	2, 3
				5	10.4	0.80[d]	2, 3
				6	14.4	0.79[d]	2
				NH		7.62[d]	2_{Ala1}
						Apdp	
				1	168.4		
				2	148.6		
				3	99.8		
				4	45.2	5.12 m	5a, Me-7, NH-4, NH-6, 2_{Asn3}, NH_{Asn3}, 2_{Ile}
				5a	36.5	2.88 m	4
				5b		1.96 m	NH-4
				6	175.0		
				Me-7	11.8	1.58 s	4, NH-4, $2_{c\text{-Asn}}$, $NH_{c\text{-Asn}}$
				NH-4		8.33 d (8.1)	4, 5b, Me-7, 2_{Ileu}
				NH-6		10.50 s	4
						c-Asn	
				1	169.1		
				2	48.8	4.71 m	3, Me-7_{Apdp}
				3	36.4	2.78 m	NH, NH-4
				4	172.1		
				NH-4		10.2 s	3, $CONH_2$
				NH		7.67[d]	3, 2_{Asn3}, NH_{Asn3}, Me-7_{Apdp}
				$CONH_2$	153.7	7.65, 7.21 s	NH-4
						Ala2	
				1	171.1		
				2	45.1	4.62 m	3, NMe$_{NMe\text{-}allo\text{-}Ile2}$
				3	17.5	1.20[d]	2, NH, NMe$_{NMe\text{-}allo\text{-}Ile2}$
				NH		7.88 br s	3, NMe$_{NMe\text{-}allo\text{-}Ile2}$

TABLE 4. Continued

	2 (*trans* isomer)				**5**		
position	δ_C[a]	δ_H[b] (*J* in Hz)	ROESY[c]		δ_C[a]	δ_H[b] (*J* in Hz)	ROESY[c]
							*N*Me-*allo*-Ile2
				1	167.4		
				2	63.6	3.95 m	1
				3	33.2	2.09 m	4, *N*Me
				4	26.5	1.59, 1.07 m	3
				5	11.2	0.87[d]	
				6	14.5	0.72[d]	*N*Me
				*N*Me	35.7	3.00 s	3, 6, 2_{Ala2}, 3_{Ala2}, NH_{Ala2}

[a]Recorded at 125 MHz; referenced to residual DMSO-d_6 at δ 39.51 ppm. [b]Recorded at 500 MHz; referenced to residual DMSO-d_6 at δ 2.50 ppm. [c]Proton showing ROESY correlation to indicated proton. [d]Signal overlapped.

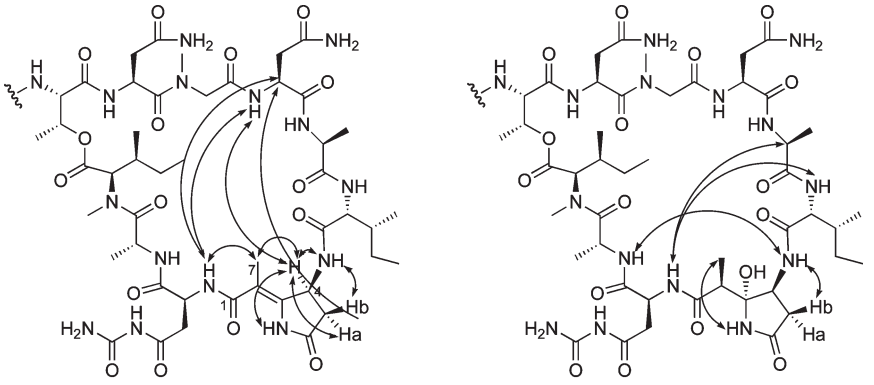

5 **7**

FIGURE 2. Comparison of ROESY correlations involving the Apdp residue in koshikamide F (**5**) and the Ahpp residue in koshikamide H (**7**).

1334 [M + H − Maa-Phe-*N*MeVal1-*N*MeAsn-*N*MeIle1-*N*-MeVal2]$^+$, and 1206 [M + H − Maa-Phe-*N*MeVal1-*N*Me-Asn-*N*MeIle1-*N*MeVal2-*N*MeLeu1]$^+$. In turn, MS/MS fragmentation of the daughter ion at *m*/*z* 1206 displayed fragments at *m*/*z* 1146 [M + H − Maa-Phe-*N*MeVal1-*N*MeAsn-*N*Me-Ile1-*N*MeVal2-*N*MeLeu1-NH_2CONH_2]$^+$ and *m*/*z* 878 [M + H − Maa-Phe-*N*MeVal1-*N*MeAsn-*N*MeIle1-*N*MeVal2-*N*Me-Leu1-Asn1-Thr-Asn2]$^+$. Thus, this fragmentation pattern was in complete agreement with the sequence obtained by NMR.

LC-MS comparisons of L- and D-FDLA derivatives of the hydrolysate of **5** (5 N HCl, 90 °C, 16 h) with authentic amino acid standards established the absolute configurations for residues D-Phe, L-*N*MeAsn, L-*N*MeLeu, L-Thr, D-Ile, L-*N*Me-Val1, and L-*N*MeVal2. Additionally, LC-MS analysis showed the presence of L- and D-enantiomers (1:1) of Ala and *N*Me-*allo*-Ile in the derivatized hydrolysate. Since we had established the L configuration for *N*Me-*allo*-Ile1 in koshikamide C, which is identical in its first seven residues to **5**, and because the NMR data for these N-terminal residues are nearly identical between the two peptides, we assigned the D configuration to *N*Me-*allo*-Ile2 in **5** by default. In the structure elucidation of koshikamide B, Araki et al. were able to establish the configuration of the Ala residues as L-Ala1 and D-Ala2 through Marfey's analysis of acid-generated peptide fragments containing only one Ala residue per fragment. Because the chemical shifts for Ala1 and Ala2 in **5** are most similar to the same residues in **8**, we have assigned the same configurations of L-Ala1 and D-Ala2 in koshikamide F. The absolute configuration of all four Asn residues (three Asn and one c-Asn) was shown to be L by chiral HPLC of an acid hydrolysate of **5**. Finally, the configuration of C-4 in the Apdp residue is proposed to be the same as in the 2-(3-amino-2-hydroxy-5-oxopyrrolidin-2-yl)propionic acid (Ahpp) residue of koshikamide B on the basis of their closely similar structural features and NMR data. Specifically, ROEs between H-4_{Apdp} (δ 5.12) and H-$5a_{Apdp}$ (δ 2.88) and between NH_{Apdp} (δ 8.33) and H-5b (δ 1.96) allowed us to propose the configuration at C-4_{Apdp} as *S*.

A second compound, koshikamide G (**6**), was present in the aqueous extract and also showed UV absorbance at 270 nm. Koshikamide G gave an [M − H]$^-$ ion at *m*/*z* 1989.0817 by HR-ESI-MS ascribable to a molecular formula of $C_{92}H_{147}N_{23}O_{26}$ indicating that **6** was 43 mass units lower than **5**. Analysis of the 2D NMR data showed koshikamide G to be the descarbamoyl analogue of koshikamide F. An insufficient quantity of **6** prevented us from performing Marfey's analysis. However, because the structures and NMR data are so similar, we assumed identical configurations for **5** and **6** at comparable chiral centers.

A final peptide present in the aqueous extract that exhibited similar chromatographic properties as **5** and **6** yet lacked an extended chromophore by UV corresponded to koshikamide H (**7**). Its molecular formula was determined to be $C_{94}H_{152}N_{24}O_{28}$ (*m*/*z* 2064.1116 [M − H]$^-$) by HR-ESI-MS and suggested the presence of an additional methylene group relative to the known koshikamide B (**8**). In fact, comparison of their NMR data indicated that the only difference was the replacement of the second amino acid residue, *N*MeVal, in koshikamide B by *N*MeIle in koshikamide H. This result was further verified by QTOF-MS fragmentation patterns that showed a difference of 14 units in fragments containing this residue. LC-MS data for the L/D-FDLA derivatives of koshikamide H hydrosylates contained peaks

corresponding to L- and D-NMe-*allo*-Ile in a 2:1 ratio. Based on sequence and NMR data similarities between cyclic koshikamides H and B and linear koshikamide D, we assumed the same configurations at comparable centers and assigned the second amino acid residue in koshikamide H as L-*N*Me-*allo*-Ile.

In addition to differences in the hydrophobic amino acids present at positions 3 and 5, cyclic koshikamides differ from one another in the substitution of the pyrrolidinone-containing unit. In these sponge collections, koshikamide F (**5**) does not appear to be a degradation product of koshikamide B (**8**) since there were no changes in the chromatographic profile during extraction and isolation, and key NMR signals diagnostic of the Apdp residue were present in freshly prepared extracts. More evidence supporting the natural occurrence of koshikamide F is obtained from the conditions under which dehydration in 2-hydroxypyrrolidones is reported to occur. Previous studies showed that for microsclerodermins, the first peptides reported to contain a 2-hydroxypyrrolidone, this residue is readily dehydrated upon exposure to trace amounts of TFA.[20] In contrast, neither koshikamide B nor H underwent dehydration under those or even stronger acid conditions. Similarly, when attempting to form the olefin of Ahpp in koshikamide B, Ariki et al. found it necessary to heat **8** at 75 °C in EtOH for 17 h to obtain the dehydration product.[4] Given the relatively strong conditions under which dehydration of Ahpp occurs when present in koshikamides, we believe it is plausible that both forms are present within this *Theonella* chemotype.

Several lines of NMR data reveal that the presence of the exocyclic olefin in the Apdp residue of koshikamide F causes significant changes in conformation of the 10-residue macrolactone when compared to Ahpp-containing peptides **7** and **8**. First, slight differences are observed for δ_H values for amino acids located within the lactone ring of koshikamide F compared to B and H (see Table S5, Supporting Information). Second, in koshikamide F the α and NH protons of Ala1, Ala2, Asn3, and Apdp along with the N^{δ} proton of c-Asn exhibited doubling in a ratio of 7:3 in DMSO-d_6, indicating koshikamide F exists as an equilibrium mixture of two conformers at room temperature. Last, strong transannular ROEs from H-4_{Apdp} to H-2_{Asn3} and NH_{Asn3}, and medium correlations from $NH_{c\text{-}Asn}$ to H-2_{Asn3} and NH_{Asn3} suggest that the sequence Asn3-Ala1-Ile-Apdp in koshikamide F adopts a β-turn conformation that brings the two halves of the macrocycle within 5 Å of one another (see Figure 2). This conformation is distinct from that of koshikamide H under the same conditions where NOEs from $NH_{c\text{-}Asn}$ to H-2_{Ala1} and NH_{Ile}, and from NH_{Ile} to NH_{Ala2} (see Figure 2 and Table S5, Supporting Information) position the β-turn-like conformation at the sequence Ala1-Ile-Ahpp-c-Asn.

With respect to the biological activities associated with linear versus Ahpp- and Ahdp-containing cyclic koshikamides, these distinct conformations are interesting. Koshikamides C, F, and H along with mutremdamide A were tested in a single round HIV-1 infectivity assay[21,22] against a CCR5-using viral envelope. Mutremdamide A and linear koshikamides failed to inhibit HIV Entry, while cyclic koshikamides F and H inhibited entry with IC_{50} values of 2.3 and 5.5 μM, respectively. Thus, the presence of the exocyclic olefin and its associated conformation appear to enhance activity relative to the hydroxypyrrolidone version. In addition, their cytotoxicity was evaluated toward the human colon tumor cell line HCT-116, a control kidney cell line (BSC-1), and the target cell line TZM-bl used in neutralization assays. Neither koshikamide F nor H showed cytotoxicity toward the target cell line cells at these concentrations. While koshikamide H was the only compound to show cytotoxicity toward a tumor cell line, in this case HCT-116 (IC_{50} =10 μM), we found this peptide to be toxic toward a control kidney cell line at similar concentrations. None of the koshikamides or mutremdamide A inhibited the growth of *Candida albicans*, and the antifungal activity of the extracts was traced to the known peptide theonellamide A.

In summary, we have isolated a new sulfated cyclic peptide and six new highly N-methylated peptides from deep-water Palauan collections of *T. swinhoei* and *T. cupola*. Mutremdamide A (**1**) contains a rare 2-amino-3-(2-hydroxyphenyl)-propanoic acid and the new N^{δ}-carbamoyl-β-sulfated asparagine residue. Compounds **2**−**7** add to the rare class of highly *N*-methylated peptides named koshikamides (two linear, koshikamide A1[23] and A2,[24] and one cyclic, koshikamide B), with koshikamides F and G being the first natural peptides to possess a 2-(3-amino-5-oxopyrrolidin-2-ylidene)-propanoic acid moiety. Thus far, it is only in deeper *Theonella* collections (averaging 100 m) such as those studied here that we have detected the presence of mutremdamide A together with koshikamides and/or theonellamides. This combination of chemistry appears to define a new *Theonella* chemotype. Interestingly, only cyclic koshikamides showed activity in HIV-1 neutralization assays suggesting the ten-residue lactone ring to be important for inhibition of HIV-1 entry. Last, the slightly more potent anti-HIV activity of koshikamide F over H may be due to the distinct conformation of the macrolactone brought about by the presence of the unsaturated pyrrolidinone residue Apdp.

Experimental Section

General Experimental Procedures. NMR spectra were recorded in DMSO-d_6 at 600 and 500 MHz using standard or cryogenically cooled triple resonance probes. DQF-COSY, 2D-HOHAHA, HSQC, HMBC, and ROESY experiments were recorded using standard pulse programs. Respective delays in HSQC and HMBC experiments were set at $^1J_{C-H}$ =145 Hz and $^{2,3}J_{C-H}$ =5, 6, and 8 Hz. Accurate mass electrospray ionization (ESI) mass spectra were measured on a time-of-flight (TOF) mass spectrometer. The instrument was operated in ω-mode at a nominal resolution of 10000. The electrospray capillary voltage was set at 2 KV and the sample cone voltage at 60 V. The desolvation temperature was set to 275 °C, and nitrogen was used as the desolvation gas with a flow rate of 300 L/h. Accurate masses were obtained using the internal reference standard method. ESI-MS/MS data were obtained using an LTQ ion

(20) (a) Bewley, C. A.; Debitus, C.; Faulkner, J. D. *J. Am. Chem. Soc.* **1994**, *116*, 7631. (b) Schmidt, E. W.; Faulkner, J. D. *Tetrahedron* **1998**, *54*, 3043. (c) Qureshi, A.; Colin, P. L.; Faulkner, J. D. *Tetrahedron* **2000**, *56*, 3679.

(21) Li, M.; Gao, F.; Mascola, J. R.; Stamatatos, L.; Polonis, V. R.; Koutsoukos, M.; Voss, G.; Goepfert, P.; Gilbert, P.; Greene, K. M.; Bilska, M.; Kothe, D. L.; Salazar-Gonzalez, J. F.; Wei, X.; Decker, J. M.; Hahn, B. H.; Montefiori, D. C. *J. Virol.* **2005**, *79*, 10108.

(22) Gustchina, E.; Bewley, C. A.; Clore, G. M. *J. Virol.* **2008**, *82*, 10032.

(23) Fusetani, N.; Warabi, K.; Nogata, Y.; Nakao, Y.; Matsunaga, S. *Tetrahedron Lett.* **1999**, *40*, 4687.

(24) Araki, T.; Matsunaga, S.; Fusetani, N. *Biosci. Biotechnol. Biochem.* **2005**, *69*, 1318.

trap mass spectrometer. Samples were infused into the mass spectrometer using a nanoelectrospray ionization system. The nitrogen gas pressure was set to 0.25 PSI and the electrospray tip voltage was set to 1.4 kV. The CID MS/MS collision energy was set to 35 V, and the parent ion isolation width was 3 Da. The maximum injection times for parent and daughter ions were 700 and 500 ms, respectively. The maximum AGC ion target setting was $1 \times 10e^5$ for parent ions and $5 \times 10e^4$ for daughter ions. QTOF-MS/MS data were obtained using a Q-TOF-2 mass spectrometer operated in positive-ion mode. The ESI capillary voltage was set to 3.5 KV, nitrogen was used as the desolvation gas with a flow of 300 L/h, with a desolvation temperature of 250 °C. Argon was used as the collision gas with a collision energy of 45 V. The parent fragment ion was generated by in-source fragmentation with a cone voltage of 40 V. Conditions used for corona discharge ESI (CDESI) detection of the sulfate group using the LCT are described in ref 17. Briefly, the ESI capillary voltage is set to 5 KV and a desolvation temperature of 500 °C is used.

Computational Details. To fully explore conformational space of the 4-MePro, MM/MD calculations at different temperatures (300, 500, 700 K) and 5 ns time steps were performed using the AMBER force field (MacroModel software package).[25] Each of the calculated structures (n =100) obtained was minimized using the Polak-Ribier Conjugate Gradient algorithm (PRCG, 1000 steps, maximum derivative less than 0.05 kcal/mol).

For the quantum mechanical calculations, both full geometry optimization and calculation of *J*-coupling values were performed using the Gaussian03 (version B.05) software package.[26] The *cis* and *trans* stereoisomers of the 4-MePro and all the staggered conformers for the *threo* and *erythro* stereoisomers of the Ahmha residues were optimized at the mPW1PW91 level of theory using the 6-31G(d) basis set; the single-point calculation of *J*-coupling was executed on the optimized geometries using the mPW1PW91 functional and the 6-31G(d,p) basis set. For the 4-MePro unit, calculations for the *cis* stereoisomer led to two significant conformers whose energies differed by 3.25 kJ (referred to in the discussion as "major" and "minor" conformers); similarly, major and minor conformers whose energies differed by 7.82 kJ were observed for the *trans* stereoisomer. Since such energy differences are relative to a fragment of the entire molecule, both the major and the minor conformers of the *cis* and *trans* stereoisomers were considered in the comparison with the experimental results.

Sponge Material. Samples of *T. swinhoei* subspecies *swinhoei* Gray, 1869, and *T. swinhoei* subspecies *verrucosa* Wilson, 1925 (lithistid Demospongiae: family Theonellidae) were collected at Mutremdiu Reef, Palau, at a depth of 100−120 m in June 2008, by scuba using mixed gases. *T. cupola* was collected on the same reef in 1997 at a depth of 90 m. Detailed taxonomic descriptions and voucher information are provided in the Supporting Information. All samples were frozen after collection and stored at −40 °C prior to extraction.

Isolation. A 6 g portion of an aqueous extract of *T. swinhoei* (PA08-05) was partitioned between *n*-BuOH−H_2O (1:1) to afford a dried *n*-BuOH extract (0.2 g). A part of this extract (120 mg) was purified by reversed-phase HPLC (Jupiter Proteo C12, 250×10 mm, 4 μm, DAD at 220 and 280 nm) eluting with a linear gradient of 65−80% MeOH in 0.05% TFA in 40 min to afford compounds **1** (10.7 mg, t_R =27.3 min), **2** (9.6 mg, t_R =22.7 min), **3** (3.7 mg, t_R =26.9 min), **4** (0.7 mg, t_R =20.0 min), **5** (4.0 mg, t_R =40.7 min), **6** (0.5 mg, t_R =42.4 min), **7** (6.6 mg, t_R =63.5 min), and **8** (20.0 mg, t_R =55.4 min). Screening by LC-MS of aqueous extracts of *T. cupola* and *T. swinhoei* subspecies *verrucosa* Wilson, 1925, was used to establish the presence of peptides **1**−**8** in aqueous extracts of these sponges.

Mutremdamide A (1): colorless amorphous powder; $[\alpha]^{23}_D$ −33.0 (c 0.1, MeOH); IR (film) ν_{max} 3335, 2965, 1674, 1619, 1542, 1456, 1244, 1204, 1131, 1086, 1026 cm^{-1}; UV (MeOH) λ_{max} (log ε) 214 (4.27), 226 (sh) (4.10), 244 (3.64), 270 (3.43) nm; ^1H and ^{13}C NMR data, see Table 1; HR-ESI-MS m/z 1068.4294 $[M + H]^+$ corresponding to a molecular formula of $C_{41}H_{65}N_{11}O_{18}S$ (calcd for $C_{41}H_{66}N_{11}O_{18}S$, 1068.4308).

Koshikamide C (2): colorless amorphous powder; $[\alpha]^{23}_D$ −97.0 (c 0.2, MeOH); IR (film) ν_{max} 3322, 2960, 2932, 1669, 1641, 1542, 1456, 1204, 1135, 722 cm^{-1}; UV (MeOH) λ_{max} (log ε) 208 (4.44), 228 (sh) (3.93) nm; ^1H and ^{13}C NMR data, see Table 4; HR-ESI-MS m/z 1431.8330 $[M + H]^+$ corresponding to a molecular formula of $C_{70}H_{110}N_{16}O_{16}$ (calcd for $C_{70}H_{111}N_{16}O_{16}$, 1431.8364).

Koshikamide D (3): colorless amorphous powder; $[\alpha]^{23}_D$ −88.5 (c 0.14, MeOH); IR (film) ν_{max} 3318, 2965, 2928, 1669, 1637, 1544, 1450, 1204, 1135, 719 cm^{-1}; UV (MeOH) λ_{max} (log ε) 208 (4.44), 228 (sh) (3.94) nm; ^1H and ^{13}C NMR data for Maa, Phe, *N*MeAsn, *N*Me-*allo*-Ile2, *N*MeVal, *N*MeLeu, Asn, Phe2, Pro, and β-Ala are identical to those reported for **2** in Table 4; ^1H NMR (DMSO-d_6, 500 MHz) *N*Me-*allo*-Ile1: δ 5.01 (1H, d, J =8.2 Hz, H-2), 1.99 (1H, m, H-3), 1.23 (1H, m, H-4a), 0.98 (1H, m, H-4b), 0.82 (3H, d, J =6. Five Hz, H-5), 0.54 (3H, d, J =6.5 Hz, H-6), 3.00 (3H, s, *N*Me), Arg: δ 4.13 (1H, m, H-2), 1.73 (1H, m, H-3a), 1.59 (1H, m, H-3b), 1.49 (2H, m, H-4), 3.09 (2H, m, H-5), 7.59 (2H, d, J- =7.8 Hz, NH-5), 8.03 (1H, d, J =7.9 Hz, NH); ^{13}C NMR (DMSO-d_6, 125 MHz) *N*Me-*allo*-Ile1: δ 168.6 (C-1), 56.4 (C-2), 32.6 (C-3), 25.4 (C-4), 10.7 (C-5), 13.4 (C-6), 29.6 (*N*Me) Arg: 173.5 (C-1), 51.4 (C-2), 28.1 (C-3), 24.9 (C-4), 40.0 (C-5), 156.5 (C-6); HR-ESI-MS m/z 1445.8514 $[M + H]^+$ corresponding to a molecular formula of $C_{71}H_{112}N_{16}O_{16}$ (calcd for $C_{71}H_{113}N_{16}O_{16}$, 1445.8521).

Koshikamide E (4): colorless amorphous powder; $[\alpha]^{23}_D$ −60 (c 0.05, MeOH); IR (film) ν_{max} 3321, 2965, 2920, 1671, 1633, 1544, 1450, 1208, 1134, 720 cm^{-1}; UV (MeOH) λ_{max} (log ε) 208 (4.44), 228 (sh) (3.94) nm; ^1H and ^{13}C NMR data for Maa, Phe, *N*MeLeu1, *N*MeAsn, *N*MeVal, *N*MeLeu, Asn, Phe2, Pro, and β-Ala are identical to those reported for **2** in Table 4; ^1H NMR (DMSO-d_6, 500 MHz) *N*MeLeu2: δ 4.93 (1H, m, H-2), 2.23 m (1H, m, H-3), 0.69 (3H, d, J =6.6 Hz, H-4), 0.78 (3H, d, J =6.6 Hz, H-5), 2.80 (3H, s, *N*Me), Arg: δ 4.02 (1H, m, H-2), 1.66 (2H, m, H-3), 1.50 (1H, m, H-3b), 1.45 (2H, m, H-4), 3.09 (2H, m, H-5), 7.60 (2H, d, J=7.8 Hz, NH-5), 7.81 (1H, d, J=7.9 Hz, NH); ^{13}C NMR (DMSO-d_6, 125 MHz) *N*meLeu2: δ 169.0 (C-1), 58.0 (C-2), 26.3 (C-3), 17.1 (C-4), 19.1 (C-5), 29.0 (*N*Me), Arg: 173.5 (C-1), 51.4 (C-2), 28.5 (C-3), 24.4 (C-4), 40.0 (C-5), 156.5 (C-6); HR-ESI-MS m/z 1417.8177 $[M + H]^+$ corresponding to a molecular formula of $C_{69}H_{108}N_{16}O_{16}$ (calcd for $C_{69}H_{109}N_{16}O_{16}$, 1417.8208).

Koshikamide F (5): colorless amorphous powder; $[\alpha]^{23}_D$ −79.1 (c 0.23, MeOH); IR (film) ν_{max} 3317, 2967, 1671, 1529, 1410, 1205, 1181, 1135, 1060, 1037, 1016, 838, 801, 722 cm^{-1}; UV (MeOH) λ_{max} (log ε) 208 (4.59), 228 (sh) (4.03), 260 (3.94), 270 (sh) (3.84) nm; ^1H and ^{13}C NMR data see Table 4; HR-ESI-MS m/z 2032.0912 $[M - H]^-$ corresponding to a molecular formula of $C_{93}H_{148}N_{24}O_{27}$ (calcd for $C_{93}H_{147}N_{24}O_{27}$, 2032.0868).

Koshikamide G (6): colorless amorphous powder; $[\alpha]^{23}_D$ −70.0 (c 0.05, MeOH); IR (film) ν_{max} 3322, 2960, 1684, 1522, 1413, 1205, 1180, 1125, 1069, 1031, 1016, 834, 802, 722 cm^{-1}; UV (MeOH) λ_{max} (log ε) 208 (4.57), 228 (sh) (4.03), 260 (3.93), 270 (sh) (3.83) nm; ^1H and ^{13}C NMR data for Maa, Phe, *N*MeVal1, *N*MeAsn, *N*Me-*allo*-Ile1, *N*MeVal2, *N*MeLeu, Asn1, Thr, Asn2, *N*MeGly, Asn3, Ala1, Ile, Apdp, Ala2, and

(25) Mohamadi, F.; Richards, N. G. J.; Guida, W. C.; Liskamp, R.; Lipton, M.; Caufield, C.; Chang, G.; Hendrickson, T.; Still, W. C. *J. Comput. Chem.* **1990**, *11*, 440.

(26) Frisch, M. J. *Gaussian 03*; Guassian, Inc., Pittsburgh, PA, 2002 (see the Supporting Information for the full reference).

*N*Me-*allo*-Ile2 identical to those reported for **5** in Table 4, ^{1}H NMR (DMSO-d_6, 500 MHz) Asn4: δ 4.60 (1H, m, H-2), 2.67 (1H, m, H-3a), 2.49 (1H, m, H-3b), 7.53 (1H, br s, NH_2-4a), 6.98 (1H, br s, NH_2-4b), 7.86 (1H, d, J =6.5 Hz, NH), ^{13}C NMR (DMSO-d_6, 125 MHz) Asn4: δ 169.1 (C-1), 49.2 (C-2), 37.2 (C-3), n.o. (C-4); HR-ESI-MS m/z 1989.0817 $[M - H]^-$ corresponding to a molecular formula of $C_{92}H_{147}N_{23}O_{26}$ (calcd for $C_{92}H_{146}N_{23}O_{26}$, 1989.0809).

Koshikamide H (7): colorless amorphous powder; $[\alpha]^{23}_D$ −84.6 (c 0.4, MeOH); IR (film) ν_{max} 3280, 2964, 1667, 1637, 1536, 1456, 1413, 1204, 1180, 1134, 1052, 1027, 1006, 833, 801, 722 cm^{-1}; UV (MeOH) λ_{max} (log ε) 206 (4.59), 226 (sh) (4.08), 260 (3.74) nm; ^{1}H and ^{13}C NMR data see Table S4 (Supporting Information); HR-ESI-MS m/z 2064.1116 $[M - H]^-$ corresponding to a molecular formula of $C_{94}H_{152}N_{24}O_{28}$ (calcd for $C_{94}H_{151}N_{24}O_{28}$, 2064.1130).

Koshikamide B (8): colorless amorphous powder; $[\alpha]^{23}_D$ −95.3 (c 1.0, MeOH); HR-ESI-MS m/z 2050.0979 $[M - H]^-$ corresponding to a molecular formula of $C_{93}H_{150}N_{24}O_{28}$ (calcd for $C_{93}H_{149}N_{24}O_{28}$, 2050.0974).

LC/MS Analysis of L/D-FDLA Derivatives. Approximately 0.5 mg of compounds **1**−**7** was separately hydrolyzed with 5 N HCl (LabChem, Inc., traceable to NIST) (0.8 mL) in an Ace high pressure tube for 16 h at 90 °C, dried, and dissolved in H_2O (100 μL). To a 50 μL aliquot of each was added 1 N $NaHCO_3$ (20 μL) and 1% 1-fluoro-2,4-dinitrophenyl-5-L-leucinamide (L -FDLA or D-FDLA solution in acetone, 100 μL), and the mixtures were heated to 40 °C for 40 min, allowed to cool to rt, neutralized with 2 N HCl (20 μL), and evaporated to dryness. Residues were dissolved in CH_3CN and analyzed by LC-MS. Analyses of the L- and L/D-FDLA (mixture of D- and L-FDLA) derivatives were performed using a C12 column (4 μm, 150 × 4.6 mm) and aqueous CH_3CN containing 0.01% TFA was used as a mobile phase eluting with a linear gradient of 25−70% CH_3CN in 40 min at a flow rate of 0.5 mL/min with mass detection (negative mode). The fragmentor and capillary voltage were kept at 70 and 1000 V, respectively, and the ion source at 350 °C. A mass range of m/z 100−1000 was scanned in 0.1 min. Retention times (t_R, min) of the FDLA-derivatized amino acids for compounds **1**: *erythro*-L-β-OHAsn 17.5, *erythro*-D-β-OHAsn 17.0, *threo*-L/D-β-OHAsn 15.1 m/z 442 $[M - H]^-$; L-*O*MeThr 23.3, D-*O*MeThr 28.5, L-*O*Me-*allo*-Thr 23.6, D-*O*Me-*allo*-Thr 27.5 m/z 426 $[M - H]^-$; L-4*S*-MePro 25.2, D-4*S*-MePro 28.3 m/z 422 $[M - H]^-$. Retention times (t_R, min) of the FDLA-derivatized amino acids for compounds **2**−**7**: L-Phe 29.5, D-Phe 33.3 m/z 458 $[M - H]^-$; L-*N*MeVal 28.3, D-*N*MeVal 32.1 m/z 424 $[M - H]^-$; L-*N*MeAsn 19.2, D-*N*MeAsn 18.0 m/z 440 $[M - H]^-$ (analyzed as *N*MeAsp); L-Pro 22.3, D-Pro 24.7 m/z 408 $[M - H]^-$; L-Arg 13.5, D-Arg 11.9 m/z 467 $[M - H]^-$; L-Thr 18.5, D-Thr 22.1 m/z 412 $[M - H]^-$; L-Ala 23.4, D-Ala 26.0 m/z 382 $[M - H]^-$; L-Ile 32.1, D-Ile 34.7 m/z 424 $[M - H]^-$. Configuration of *N*Me-*allo*-Ile and *N*MeLeu residues were established by LC-MS analysis using a reversed-phase C18 column (4 μm, 250 × 4.6 mm) and a linear gradient of 3:1 20 mM ammonium formate buffer (AF)/CH_3CN to 3:7 AF/CH_3CN over 40 min. Retention times (t_R, min) of the FDLA-derivatized amino acids for compounds **2**−**7**: L-*N*MeLeu 22.6, D-*N*MeLeu 27.3 m/z 438 $[M - H]^-$; L-*N*MeIle 22.4, D-*N*MeIle 28.1 m/z 438 $[M - H]^-$; L-*N*Me-*allo*-Ile 22.3, D-*N*Me-*allo*-Ile 29.1 m/z 438 $[M - H]^-$.

Chiral HPLC Analysis. The acid hydrosylates of **1**−**7** (0.3 mg) were analyzed by chiral HPLC eluting with 1 mM $CuSO_4$/MeCN (95:5) at a flow rate of 0.5 mL/min, with UV detection at 254. The retention times of Asp were compared to authentic standards whose retention times were 15.5 min for L-Asp and 19.9 min for D-Asp.

Biological Assays. Cytotoxicity assays were carried out in duplicate using an MTT-based colorimetric cell proliferation assay. Briefly, HCT-116, BSC-1, or TZM-BL cells were seeded in 96-well tissue culture plates at a density of 2×10^4 cells/well in 50 μL of growth media and allowed to adhere for 18 h. Attached cells were incubated with inhibitors for 24 h (as controls for the neutralization assay), after which the media was either replaced or diluted 3-fold with fresh growth media. Following an additional 48 h incubation period, cell viability was assessed upon treatment with MTT and absorbance readings. Single round HIV-1 neutralization assays were performed in duplicate with viruses pseudotyped with SF162 Envelope using published protocols.[21]

Acknowledgment. We thank H. Baker for HIV-1 neutralization assays; the AIDS Research and Reference Reagent Program, Division of AIDS, NIAID, NIH, for reagents and cell lines used in the HIV-1 neutralization assays; and M. Kelly and the National Cancer Institute for identification of *T. cupola*. The underwater photograph of *T. swinhoei* was provided by co-author P. L. Colin, and the cover art was designed by M. Garraffo. This work was supported by the Intramural AIDS Targeted Antiviral Program, Office of the Director, NIH (C.A.B.), and the NIH Intramural Research Program (NIDDK).

Note Added after ASAP Publication. In reference 26, the spelling of the authors name was corrected, the corrected version reposted April 21, 2010.

Supporting Information Available: Complete ref 26, 1D and 2D ^{1}H,^{1}H and ^{1}H,^{13}C NMR data used for structure elucidation of compounds **1**−**7**, mass spectra for compounds **1**−**8**, and taxonomic descriptions of *T. swinhoei* subspecies. This material is available free of charge via the Internet at http://pubs.acs.org.